JOURNAL OF MATERIALS SCIENCE 29 (1994) 5199–5206

Flexural strength, fracture toughness and fatigue crack growth behaviour of chromium alloyed γ-base TiAl

R. GNANAMOORTHY, Y. MUTOH
Department of Mechanical Engineering, Nagaoka University of Technology, Nagaoka, Japan
N. MASAHASHI, Y. MIZUHARA
Nippon Steel Corporation, Kawasaki, Japan
M. MATSUO
JATIS, Chiyoda-ku, Tokyo, Japan

Mechanical properties of γ-base titanium aluminides strongly depend on microstructural parameters. Flexural strength, fracture toughness and fatigue crack growth properties were estimated for the cast and heat-treated (HT-TiAlCr) and cast, heat treated and isothermal forged (ITF-TiAlCr) chromium alloyed γ-base titanium aluminides at room temperature. HT-TiAlCr possessed superior fracture properties compared to ITF-TiAlCr. Toughening due to microcracks, and crack bridging by uncracked ligaments were observed in the test materials. Presence of lamellar grains in HT-TiAlCr increased the crack growth resistance and contributed positively to fracture properties. The coarse grain size promoted large crack deflection and fracture surface mismatch and caused high levels of crack closure in HT-TiAlCr. Combined crack-tip blunting and bridging by ductile β-phase was significant in the case of ITF-TiAlCr. Fracture mechanisms of test materials were investigated and correlated to the fracture properties.

1. Introduction

Attractive mechanical properties and the light weight of titanium aluminide base intermetallic compounds make them most suitable for applications in the aerospace and automobile industries [1–3]. Among titanium aluminides, γ-phase materials are of special interest because they have higher oxidation resistances, higher elastic modulii and better creep properties than α_2-phase titanium aluminides. But, their low room temperature ductility and poor formability restrict any industrial application. Many investigations have shown the strong dependence of mechanical properties of γ-phase titanium aluminides on microstructure [3], alloying additions [4–6] and processing conditions [7]. Addition of ternary elements such as chromium [4], manganese [5] and vanadium [6] were found to have considerable influence on the mechanical properties of titanium aluminides. Chromium alloyed γ-base titanium aluminides possess high ductility [4] and fracture toughness [8]. Still, the maximum room temperature ductility and toughness achieved are below the acceptable limits for practical applications. There is growing interest in developing titanium aluminide intermetallics with improved mechanical properties through advanced processing conditions [3, 7]. Materials processed through conventional ingot metallurgy, casting and powder metallurgy techniques are subjected to subsequent hot working to result in a fine grained homogeneous microstructure. Isothermal forging (ITF) results in a fine, homogeneous material compared to hot extrusion techniques [3].

As these materials are most suitable for applications in rotating turbine structures and other structural components, their fatigue and fracture characteristics must be understood before using them in practice. The fracture mechanism of binary titanium aluminides has been investigated in detail [9–12], while that of ternary titanium aluminides needs considerable attention. Very little research has been carried out on the fatigue crack growth behaviour of the titanium aluminide base intermetallic compounds [13, 14]. In particular, the study of the fatigue crack propagation and its relation to alloy composition, microstructure and processing conditions for γ-base titanium aluminides needs considerable work. It is widely recognized that fatigue crack closure plays a significant role in determining the fatigue crack growth rates. The crack closure mechanism and the influence of microstructural parameters on the crack closure mechanism of the γ-base titanium aluminides are not understood in detail.

In the present study, the fracture behaviour of cast and heat-treated (HT), and cast, heat-treated and ITF chromium alloyed γ-base titanium aluminide base intermetallic compounds are investigated. Microstructural controlled γ-base titanium aluminides containing ductile β (b.c.c)-phase have shown high ductility

0022–2461

[15] and were used in the current investigation. Fracture toughness and fatigue crack growth behaviour were estimated. The influence of microstructural parameters on the fracture toughness and the fatigue crack growth properties of γ-base chromium alloyed titanium aluminides are discussed.

2. Experimental procedure

2.1. Test materials

γ-base Ti-47 at %, Al-3 at % Cr alloys used in the present investigation were prepared from high purity ingots by plasma arc melting and casting. The nominal composition of the test materials are shown in Table I. The ingots were homogenized for 96 h at 1050 °C in vacuum and fabricated into cylindrical rods (35 mm in diameter and 42 mm long) for ITF. The ITF was carried out in vacuum at temperatures >1200 °C and at low strain rates for obtaining fine grained structures. Heat-treated TiAlCr contained mostly equiaxed γ-grains and some regions of lamellar α_2-grains with an average grain size of about 60 μm. X-ray diffraction (XRD) studies carried out on the samples indicated the presence of β-phase in addition to α_2 and γ-phases. Detailed TEM investigations performed by Hanamura *et al.* [16] also confirmed the presence of a third phase (β-b.c.c.) in HT-TiAlCr. Fine homogeneous equiaxed grains with an average grain size of ≈ 18.5 μm were obtained after ITF of cast and heat-treated material. ITF-TiAlCr contained only two phases, γ and β. Test specimens were made by multiwire cutting and then machining to required dimensions and surface finish.

2.2. Flexural strength experiments

Flexural strengths of test materials were estimated using three-point bend specimens of dimensions $3 \times 4 \times 35$ mm^3 (Fig. 1a) at room temperature. The span length of three-point bending was 30 mm. Experiments were conducted using an Instron type universal testing machine at a crosshead speed of 0.5 mm min^{-1}. Fractographical investigations were carried out on the fractured surfaces using scanning electron microscopy (SEM).

2.3. Fracture toughness experiments

The plane strain fracture toughness, K_{Ic}, tests using specimens of dimensions $5 \times 10 \times 55$ mm^3 (Fig. 1b) were carried out according to the ASTM standard [17]. The valid fracture toughness value was obtained only for ITF-TiAlCr. Then, the elastic–plastic fracture toughness, J_{Ic}, tests using specimens with side-grooves were also carried out for test materials according to the convenient J_{Ic} test technique, which is based on the maximum load in the load–displacement plot of the specimen with proper depths of side-grooves and where the precrack coincides with the crack initiation point [18]. EDM notch was used as a starter for the fatigue precracking of three-point bend specimens. A fatigue crack was introduced up to a/W ratio of about 0.55 using a sinusoidal wave of 10 Hz and stress ratio of 0.1. The final maximum stress intensity factor for fatigue cracking (K_{fmax}) was controlled at lower than $0.6K_{Ic}$. Side-grooves were introduced in the precracked specimen using a fine diamond cutter of 0.3 mm thickness to a depth of about 25% of the specimen thickness. These fatigue crack lengths and side-groove depths ensured that the maximum load point coincided with the crack initiation point [18].

TABLE I Composition of plasma arc melted TiAlCr alloy

Element	Ti (at %)	Al	Cr	O (wt p.p.m.)	H	C
	48.1	49.2	2.75	250	7	120

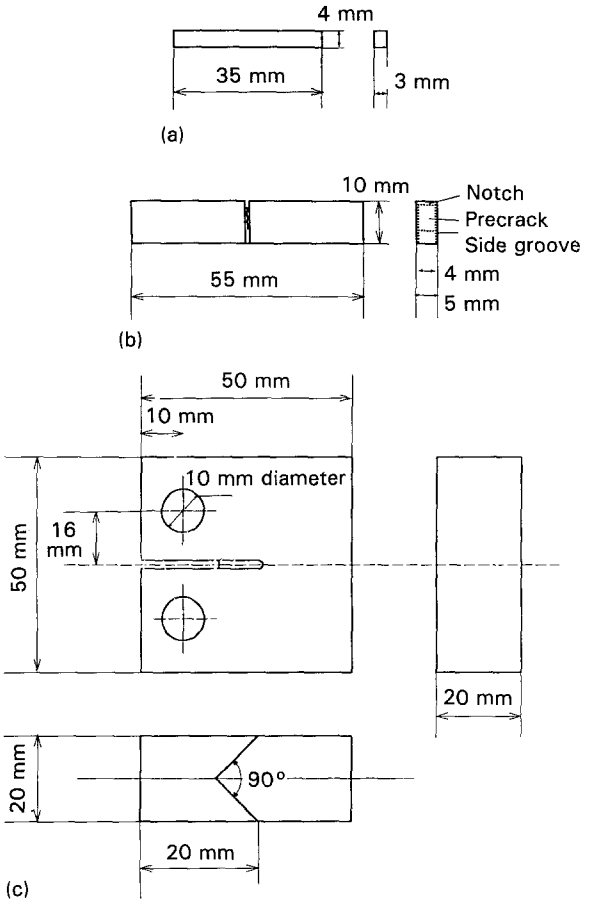

Figure 1 Geometry of test specimens. (a) Three-point bend specimen; (b) side-grooved toughness specimen; (c) chevron-notched CT specimen.

In addition, fracture toughness tests using 20 mm thick CT specimens (Fig. 1c) were conducted for HT-TiAlCr. Chevron-notched CT specimens were fatigue precracked and fracture toughness values were estimated according to the ASTM test standard for evaluating the plane strain fracture toughness K_{Ic} [17].

2.4. Fatigue crack growth experiments

Fatigue crack growth data were generated from four-point bend specimens of dimensions $5 \times 10 \times 55$ mm^3, whose sides were sufficiently polished to study the crack path. EDM notch was used as a starter for the fatigue cracking. Test specimens were precracked in three-point bending up to a crack length of about 3 mm to avoid the mechanical effect of notch. Cyclic

bending loads were applied with initial ΔK values of about 2 MPa $m^{1/2}$ to the specimen and incremented by 0.25 MPa $m^{1/2}$ until crack growth was observed. Crack length measurements were made using a travelling microscope with an accuracy of 10 μm. Cyclic fatigue crack propagation experiments were carried out using a sinusoidal wave of 10 Hz and stress ratio of 0.1 in a controlled room-air (20 °C, 55% relative humidity) atmosphere. Crack closure measurements based on the unloading elastic-compliance techniques were carried out using back-face strain gauge. Fractured specimens were cut using a fine diamond cutter and the sub-surface below the crack path and profile were studied using optical and scanning electron microscopes on the metallographically prepared specimens at the mid-specimen thickness region.

3. Results

The characteristic values for flexural strength, fracture toughness and fatigue crack growth curve of test materials are summarized in Table II. The flexural strength of ITF-TiAlCr was 713 MPa, while that of HT-TiAlCr was 748 MPa. ITF fine grained microstructure contributed negatively to flexural strength.

Fracture toughness tests using 20 mm thick HT-TiAlCr chevron notched CT specimens, the thickness of which did not satisfy the requirement for plane strain fracture toughness [16], yielded an average value of 34.8 MPa $m^{1/2}$. Conservative fracture toughness values were obtained from thin side-grooved three-point bend specimens (32.01 MPa $m^{1/2}$). The J_{Ic} fracture toughness estimated using side-grooved specimens yielded an average value of 12.8 kJ m^{-2}.

TABLE II Characteristic values for flexural strength fracture toughness and fatigue crack growth curves

	HT-TiAlCr	ITF-TiAlCr
Flexural strength (MPa)	748	713
Fracture toughness		
K_{Ic} MPa $m^{1/2}$	34.8[a]	12.2
J_{max} (KJ m^{-2})	12.8	1.4
Fatigue crack growth curve		
ΔK_{th} (MPa $m^{1/2}$)	9.5	7.6
ΔK_t (MPa $m^{1/2}$)	10.5	8.0
Slope m in Paris regime	14.0	36.0

[a] K_c value.

Estimated plane strain fracture toughness values (K_{Ic}) from three test specimens for ITF-TiAlCr were 12.0, 12.7 and 11.8 MPa $m^{1/2}$. The J_{Ic} fracture toughness estimated using the side-grooved single specimen techniques yielded an average value of 1.41 KJ m^{-2} for ITF-TiAlCr. Estimated values from three specimens tested were 1.44, 1.40 and 1.40 kJ m^{-2}. The scatter in the test results was less compared to the HT-TiAlCr.

Fracture surface of fracture toughness of the HT-TiAlCr specimen was extremely rough compared to the ITF-TiAlCr specimen (Fig. 2). Room temperature fracture surfaces of test materials exhibited a dominant transgranular cleavage type of fracture both in the fatigue precrack and unstable fracture regions. Lamellar fracture regions were dominant in the HT-TiAlCr material, as shown in Fig. 3a. Some intergranular fracture regions were also observed in ITF-TiAlCr (Fig. 3b).

Fatigue crack growth curves of test materials are shown in Fig. 4. The values of ΔK_{th} and slope m in crack growth curves are listed in Table II. The heat-treated material had a higher fatigue threshold stress intensity factor range (ΔK_{th}) compared to the ITF material. The slope m of ΔK versus da/dN curve in the Paris regime for the ITF-TiAlCr was very high compared to HT-TiAlCr. The ratio of K_{cl}/K_{max} as a function of ΔK is shown in Fig. 5. At near-threshold values high crack closure levels were observed for test materials. The crack closure level decreased with increasing stress intensity factor range for HT-TiAlCr. Based on the crack closure measurements, the estimated effective stress intensity factor range (ΔK_{eff}) versus crack growth rate for the test materials are shown in Fig. 6. The effective stress intensity factor range versus crack growth rate data almost approached

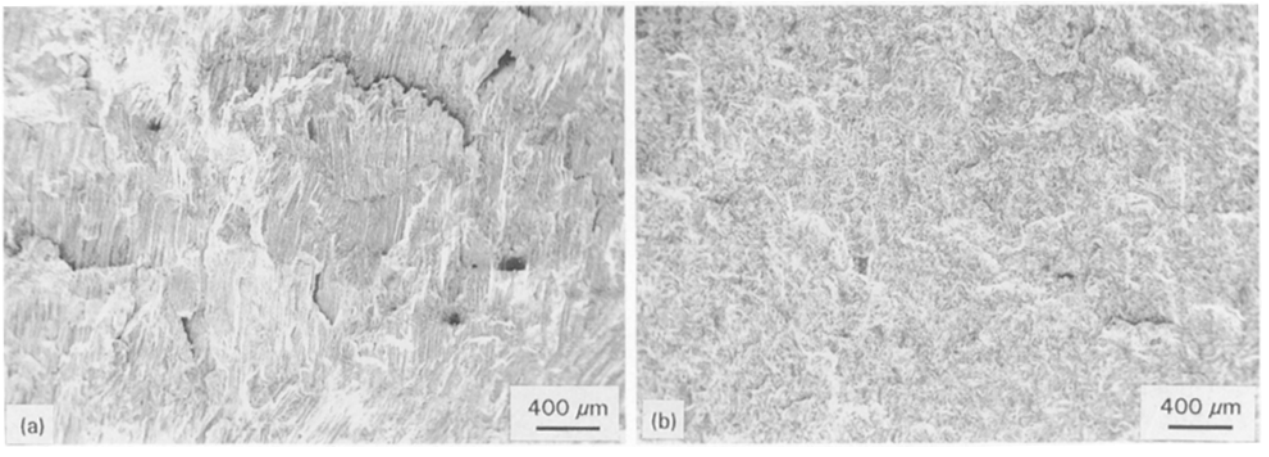

Figure 2 Low magnification view of fracture surfaces of fracture toughness specimens. (a) HT-TiAlCr; (b) ITF-TiAlCr.

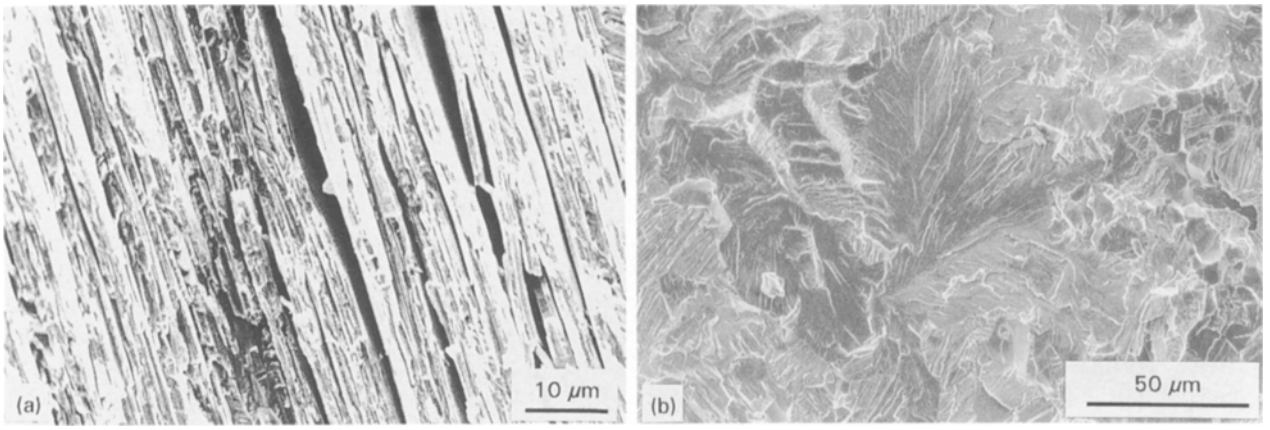

Figure 3 Fractographs of fracture toughness specimens. (a) HT-TiAlCr; (b) ITF-TiAlCr.

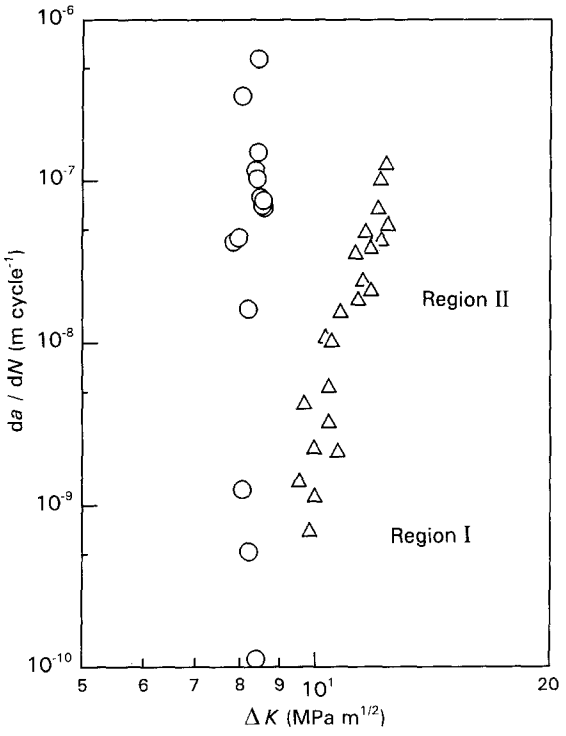

Figure 4 Stress intensity factor range (ΔK) vs crack growth velocity (da/dN) for test materials. △, HT-TiAlCr; ○, ITF-TiAlCr.

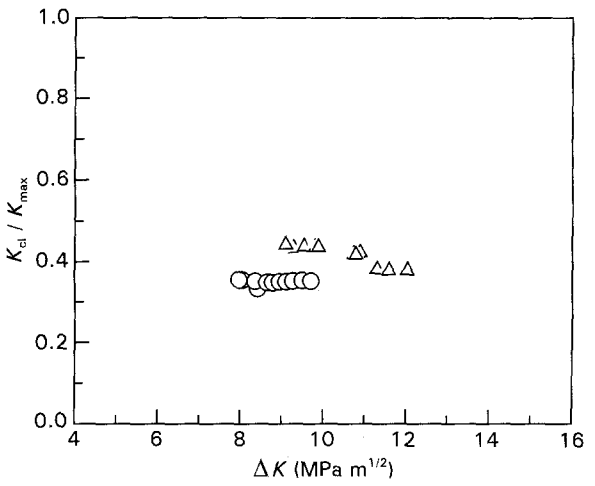

Figure 5 K_{cl}/K_{max} vs ΔK for test materials. △, HT-TiAlCr; ○, ITF-TiAlCr.

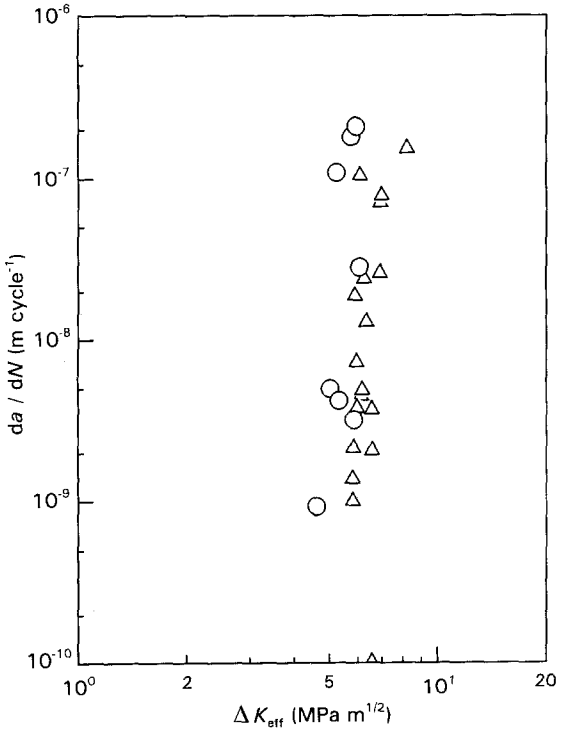

Figure 6 Effective stress intensity factor range (ΔK_{eff}) vs crack growth velocity (da/dN) for test materials. △, HT-TiAlCr; ○, ITF-TiAlCr.

each other. However, the crack growth rates for HT-TiAlCr were low compared to those for ITF-TiAlCr. This indicated that other factors, such as stress shielding may have been more significant in HT-TiAlCr.

From the fatigue crack growth experimental results it was clear that crack closure played a significant role in fatigue crack growth behaviour of the γ-base titanium aluminides. During fatigue crack propagation several crack closure mechanisms could operate [19]. In order to identify the dominant toughening mechanism detailed analysis of the crack path was carried out using optical and scanning electron microscopes. The fracture path of the toughness specimens are shown in Fig. 7. The fracture path of HT-TiAlCr was very tortuous compared to ITF-TiAlCr. Average values of lineal roughness (the ratio between the actual profile length and the projected profile length) and

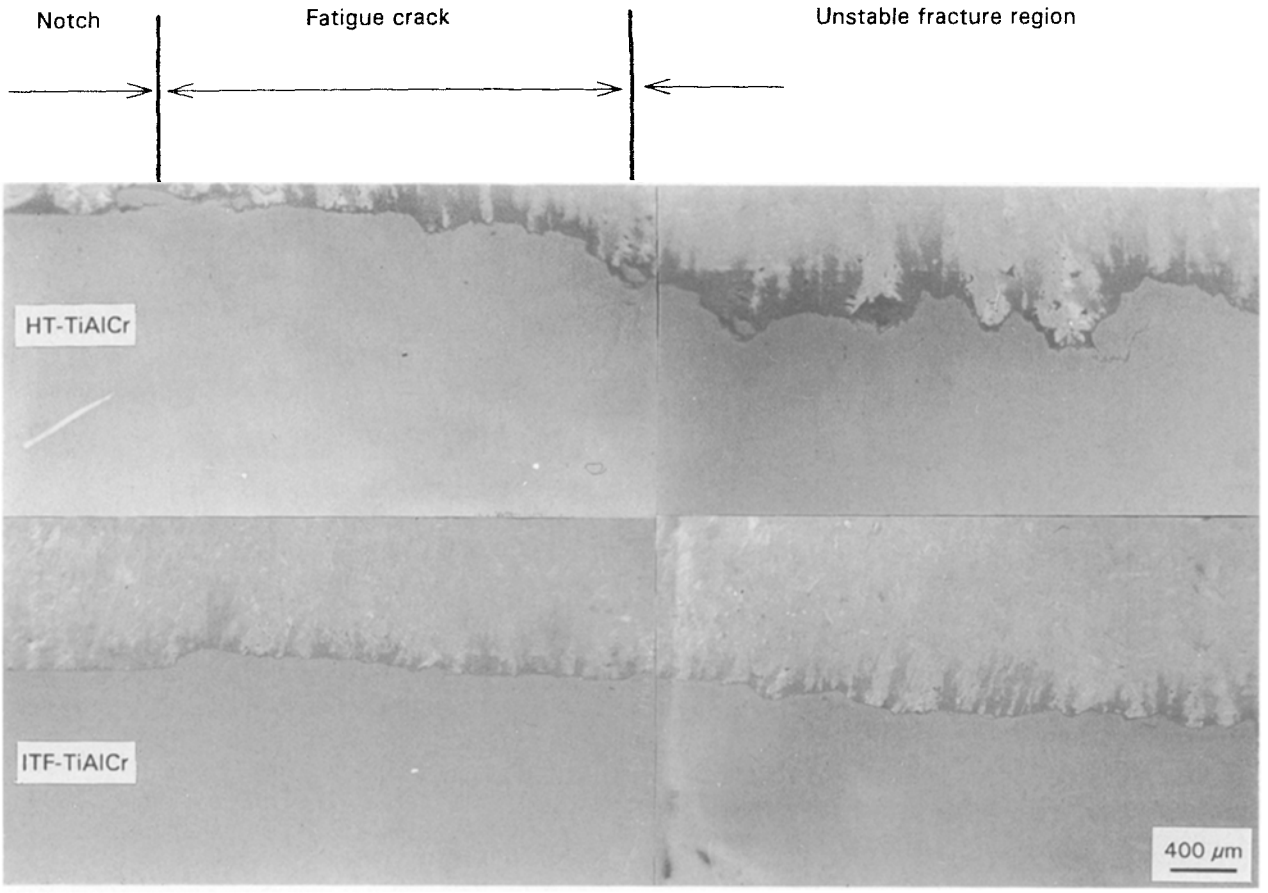

Figure 7 Fracture path in fracture toughness specimens.

TABLE III Fatigue crack profile parameters

	HT-TiAlCr	ITF-TiAlCr
Lineal roughness	1.182	1.037
Deflection angle, θ°	30–60	25–35
Average value of θ	45.13	30.50
$(D/D + S)$ parameter	0.352	0.111

deflection angle measured from a large number of profile tracings obtained from optical and scanning electron microscope views on the fatigue crack region of the test materials are shown in Table III. These values represent the fracture path tortuosity quantitatively. Lineal roughness and deflection angle of HT-TiAlCr were very high compared to those of ITF-TiAlCr.

A large number of microcracks were observed in the crack tip region of HT-TiAlCr and ITF-TiAlCr indicating the contribution of microcrack toughening in the case of two-phase titanium aluminides irrespective of the microstructure (Fig. 8a). In addition, uncracked ligaments (Fig. 8b) and crack branching (Fig. 8c) were also observed in the materials investigated.

In the case of HT-TiAlCr the fatigue crack path morphology indicated the contribution to crack closure from crack deflection (Fig. 9a) and fracture surface mismatch (Fig. 9b). Significant asperity contacts (Fig. 9b), which resulted from crack deflection, contributed to crack closure in HT-TiAlCr. This was consistent with higher levels of crack closure in HT-TiAlCr compared to ITF-TiAlCr. Crack bridging by uncracked ligaments was also observed in ITF-TiAlCr (Fig. 10). From the size of the uncracked ligaments (about 1 or 2 μm), it was possible that the presence of β-grains along the crack path might have caused this type of crack-tip blunting and bridging in the case of ITF-TiAlCr.

4. Discussion

The microstructural parameters, such as the amount of second phase [20–22], grain size [23] and orientation of lamellar grains [22], had a strong influence on the fracture properties of γ-base titanium aluminides. Influence of these factors on the fracture properties of HT-TiAlCr and ITF-TiAlCr are discussed in the following sections.

4.1. Cast and heat-treated TiAlCr

Cast and heat-treated chromium alloyed γ-base titanium aluminides contained regions of hard α_2 lamellar grains in equiaxed γ-matrix. Far fewer ductile β-grains were observed. From the experimental results, it was clear that the flexural strength, fracture toughness and fatigue crack growth behaviour of HT-TiAlCr were superior compared to ITF-TiAlCr. The lamellar grains in HT-TiAlCr offered high resistance to crack propagation and improved the fracture properties. It is well reported that the fracture of titanium aluminides occurs by microcrack nucleation, growth and

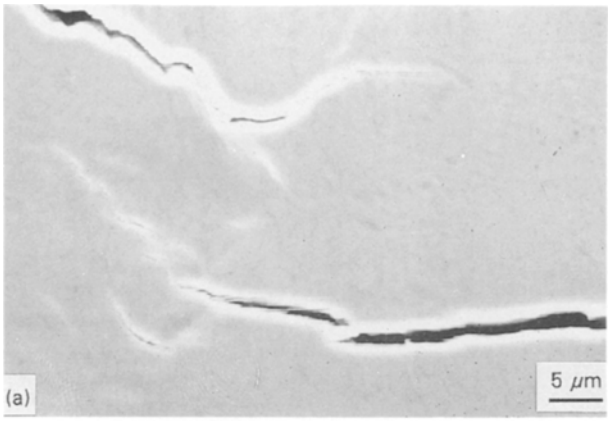

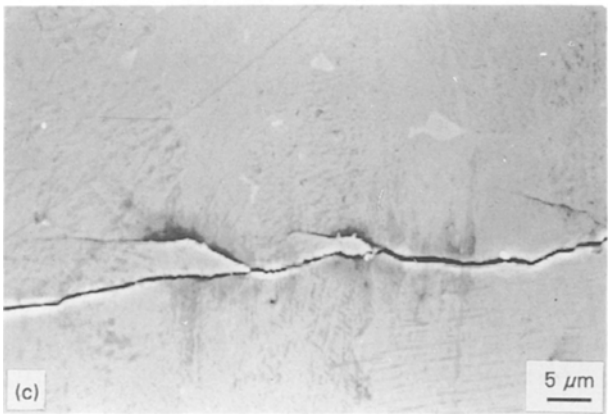

Figure 8 Fracture crack path morphology of test materials. (a) Microcracking and bridging in HT-TiAlCr; (b) uncracked ligaments in HT-TiAlCr; (c) crack branching in ITF-TiAlCr.

coalescence [22, 24]. A large number of microcracks were observed in the crack-tip region during the present investigation. Microcracks nucleated at the interphase, and/or grain boundaries, propagated and resulted in the final lamellar fracture regions (Fig. 3a). Large amounts of energy consumed in tearing hard lamellar laths and relaxation of stresses due to microcracking resulted in increased fracture toughness. The presence of hard lamellar grains in the crack path also caused crack deflection and branching and increased the fatigue crack growth resistance for HT-TiAlCr. Meanwhile, HT-TiAlCr contained ductile b.c.c. β-phase in addition to α_2- and γ-phases. The high resistance to fracture of the hard α_2-phase and/or the presence of transformed ductile β-phase [15, 16] contributed to the fracture toughness and fatigue crack growth resistance of HT-TiAlCr.

Distinct Region I and Region II fatigue crack growth behaviour was observed for HT-TiAlCr similar to metallic materials [27], as shown in Fig. 4. The coarse grained HT-TiAlCr possessed a higher fatigue threshold stress intensity factor range (ΔK_{th}) than fine grained ITF-TiAlCr. Very high crack closure was observed for HT-TiAlCr in the near-threshold region and it decreased with an increasing applied stress intensity factor range. A rough crack path was observed for HT-TiAlCr compared to ITF-TiAlCr. Large numbers of microcracks were observed in this material indicating the dominant contribution of microcrack toughening. In addition, crack branching and crack bridging were also observed. (Fig. 8).

The fracture surface of HT-TiAlCr was very rough compared to the nearly flat fracture surface of ITF-TiAlCr. The fatigue crack was deflected when it encountered lamellar grains and/or grain boundaries (Fig. 9a) and resulted in a tortuous crack path (Fig. 7). The crack path morphology investigations indicated high lineal roughness for HT-TiAlCr compared to ITF-TiAlCr as shown in Table III. The extent of crack path tilting expressed in terms of $D/D + S$, where D is the distance over which the tilted crack advances along the kink and S is the distance over which Mode I crack growth occurs in each segment (after Ref. 25), was also very high in HT-TiAlCr compared to ITF-TiAlCr. So, it was evident that the contribution of roughness induced crack closure was significant in the case of HT-TiAlCr. Asperity contacts contributing to high roughness induced crack closure observed along the crack path in the near-threshold region (Fig. 9b) were consistent with the above analysis. The contribution due to this type of crack closure was less in the high stress intensity factor range region.

4.2. ITF TiAlCr

Subsequent isothermal forging of cast and heat-treated TiAlCr resulted in a fine homogeneous microstructure with improved tensile properties [15]. The ITF material contained ductile β-phase in the γ-matrix. No lamellar grains were observed after ITF [15].

The fracture properties of the ITF material were inferior compared to cast and heat-treated materials. The main source of fracture toughness in the case of ITF-TiAlCr could be attributed to the presence of ductile β-phase. Absence of hard lamellar grains, which offer high resistance to crack propagation in HT-TiAlCr, resulted in low toughness values in the case of ITF-TiAlCr.

The fatigue crack growth curve of ITF-TiAlCr was similar to that of brittle ceramics [26]. No distinct Region I and Region II were observed. The near-threshold fatigue crack growth region was very steep for both materials and fatigue crack growth rates decreased with increasing grain size. The behaviour was similar to that in steel [27]. The transition stress intensity factor range (ΔK_t) from Region I to Region II seemed to depend strongly on the microstructural

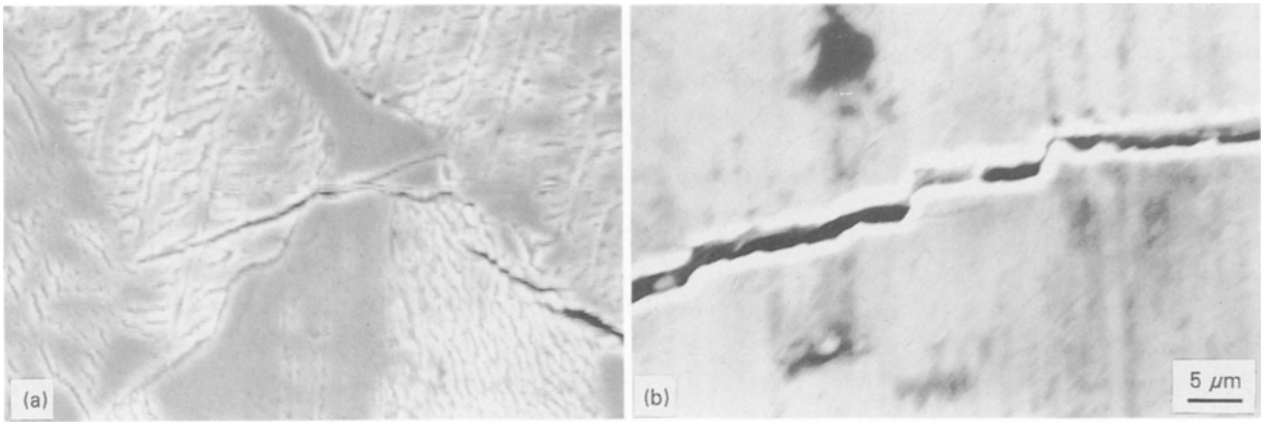

Figure 9 Fatigue crack path morphology of HT-TiAlCr. (a) Crack deflection; (b) asperity contacts.

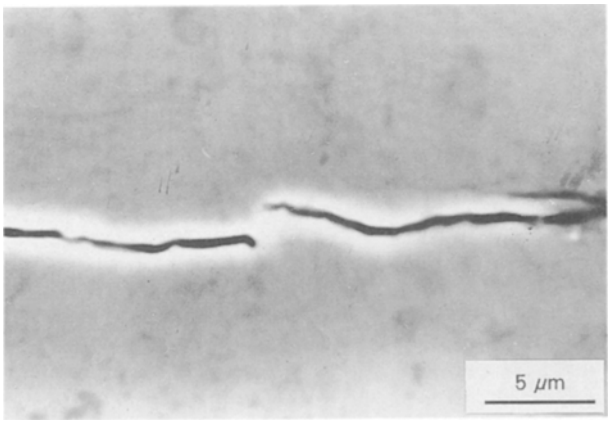

Figure 10 Fatigue crack path morphology of ITF-TiAlCr. Uncracked ligaments due to β-phase.

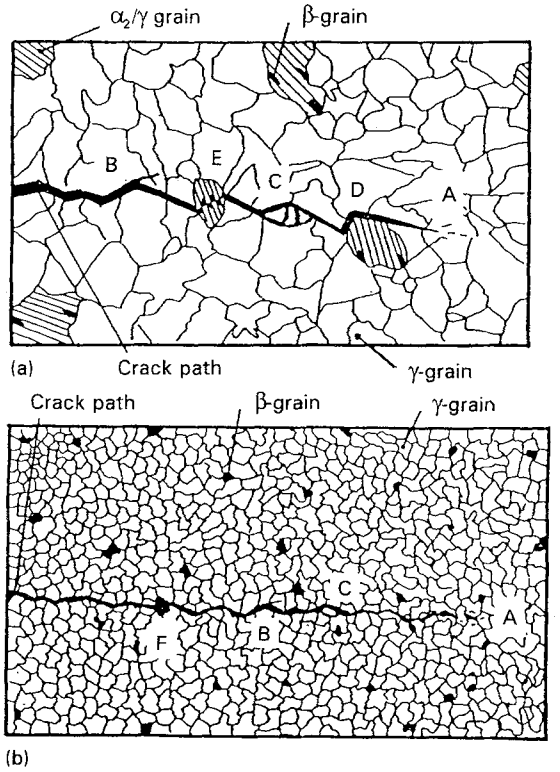

Figure 11 Schematic representation of fatigue crack path in (a) HT-TiAlCr and (b) ITF-TiAlCr. Toughening due to microcracking, crack branching, crack bridging, crack deflection at grain boundary, lamellar grains, and ductile β-phase are shown as A, B, C, D, E and F, respectively.

parameters, again similar to steels [27]. Notable reduction in the Region II crack growth rates were observed for the coarse grained HT-TiAlCr. From the experimental results it was clear that the microstructural parameters played a significant role in the Region II crack growth behaviour of titanium aluminide intermetallics.

The crack path of ITF-TiAlCr was more or less straight resulting in a flat fracture surface. Microcracks were observed in the crack-tip region as shown in Fig. 8a. In addition, crack branching and crack bridging by uncracked ligaments were also observed in ITF-TiAlCr. This indicated that the major toughening mechanisms in the case of γ-base titanium aluminides were stress shielding due to microcracking, crack bridging and crack branching irrespective of the microstructure. This was consistent with high levels of crack closure observed in the γ-base titanium aluminides investigated. The possible contribution due to each of the above toughening mechanisms are given in Table IV.

From the crack path morphology investigations it was clear that the contribution of roughness induced crack closure was less significant or absent in the case of ITF-TiAlCr. Fine grain size of ITF-TiAlCr caused less crack path deflection compared to the coarse grained HT-TiAlCr. But, combined crack-tip blunting and bridging was observed in the case of ITF-TiAlCr, as shown in Fig. 10. This might have resulted from the presence of large amounts of ductile β-grains and contributed to high closure.

Summarizing the foregoing observations and discussions, the fatigue crack paths in HT-TiAlCr and ITF-TiAlCr are schematically illustrated in Fig. 11. In the figure, the factors contributing to crack closure and stress shielding are indicated as A, microcracking; B, crack branching; C, crack bridging by interstitial particles; D, crack deflection; E, resistance due to hard lamellar grains; F, crack-tip blunting and bridging by the β-phase. Toughening due to mechanisms indicated by A, B and C are common to γ-base titanium aluminides. Large amount of crack deflection (D) and resistance due to hard lamellar grains (E) are specific to

TABLE IV Toughening mechanisms in chromium alloyed γ-base titanium aluminides

	HT-TiAlCr	ITF-TiAlCr
Microcrack shielding	D	D
Crack bridging by uncracked ligaments	D	D
Crack path deflection	D	N
Asperity contacts	D	N
Crack-tip blunting	I	D
Combined crack-tip blunting and bridging by β-grains	N	D

D, Dominant; I, influential; N, not observed.

HT-TiAlCr. Crack-tip blunting and bridging by ductile β-phase (F) was observed only for ITF-TiAlCr.

5. Conclusions

Flexural strength, fracture toughness and fatigue crack growth behaviour of cast and heat-treated and subsequently ITF chromium alloyed γ-base titanium aluminides, were investigated. Based on the above investigations, the following conclusions are made:

1. Microstructure had a strong influence on the mechanical properties of chromium alloyed γ-base titanium aluminides. The fracture toughness and fatigue crack growth properties strongly depended on the microstructure and grain size.
2. Coarse grained HT-TiAlCr possessed excellent fracture toughness and superior fatigue crack growth properties compared to ITF-TiAlCr. Stress shielding due to microcracking, crack branching and crack bridging by uncracked ligaments were dominant toughening mechanisms in γ-base titanium aluminides. In addition, in the case of HT-TiAlCr, the presence of lamellar grains in the equiaxed matrix caused extensive crack deflection and increased resistance to fracture. Roughness induced crack closure played a significant role in HT-TiAlCr.
3. In ITF-TiAlCr, combined crack-tip blunting and bridging by ductile β-phase was the dominant mode of the toughening mechanism.

Acknowledgements

The authors acknowledge the experimental assistance provided by M. Takahashi and A. Hayashi. Support for one of the authors (RG) from the Ministry of Education, Science and Culture, Japan, is gratefully acknowledged.

References

1. H. A. LIPSITT, *Proc. Mater. Res. Soc. Symp.* **39** (1985) 351.
2. G. SAUTHOFF, *Z. Metallkd.* **80** (1989) 337.
3. Y. W. KIM, *J. Metals* **41** (1989) 24.
4. S. C. HUANG and E. L. HALL, *Met. Trans. A.* **22A** (1991) 2619.
5. T. HANAMURA, R. UEMORI and M. TANINO, *J. Mater. Res.* **3** (1988) 256.
6. S. C. HUANG and E. L. HALL, *Acta Metall.* **39** (1991) 1053.
7. S. SEN and D. M. STEFANESCU, *J. Metals* **43** (1991) 30.
8. R. GNANAMOORTHY, Y. MUTOH, N. MASAHASHI and M. MATSUO, unpublished work.
9. S. A. COURT, V. K. VASUDEVAN and H. L. FRASER, *Phil. Mag. A.* **61** (1990) 141.
10. H. A. LIPSITT, D. SCHECHTMAN and R. E. SCHAFRIK, *Met. Trans. A* **6A** (1975) 1991.
11. D. SCHECHTMAN, M. J. BLACKBURN and H. A. LIPSITT, *Met. Trans. A.* **5A** (1974) 1373.
12. G. HUG, A. LOISEAU and P. VEYSSIERE, *Phil. Mag. A.* **57** (1988) 499.
13. W. O. SOBOYEJO, J. E. DEFFEYES and P. B. ASWANTH, *Mater. Sci. Engng. A* **138** (1991) 95.
14. S. MALL, E. A. STAUBS and T. NICHOLAS, *Trans. ASME: J. Engng. Mater. Tech.* **112** (1990) 435.
15. N. MASAHASHI, Y. MIZUHARA, M. MATSUO, K. HASHIMOTO, M. KIMURA, T. HANAMURA and H. FIJI, in "Proc. symp. mat. res. soc." **213** (1991) 795.
16. T. HANAMURA, N. MASAHASHI, Y. MIZUHARA, M. MATSUO and H. MORIKAWA in "Proc. spring meeting of JIM" (The Japan Institute of Metals, 1992) p. 320.
17. ASTM E399-81, in "1981 Annual book of ASTM standards, Part 10" (American Society of Testing Materials, 1981) p. 592.
18. Y. MUTOH, in "Role of fracture mechanics in modern technology"(Elsevier, North Holland, 1987) p. 503.
19. A. J. MCEVILY, in "Mechanics of fatigue crack closure, ASTM STP 982" (American Society of Testing Materials, 1988) p. 35.
20. W. O. SOBOYEJO, D. S. SCHWARTZ and S. M. L. SASTRY, *Met. Trans. A.* **23A** (1992) 2039.
21. S. L. KAMPE, P. SADLER, D. E. LARSEN and L. CHRISTODOULOU, in "Microstructure/property relationships in titanium aluminides and alloys" (The Minerals, Metals, & Materials, 1991) p. 313.
22. S. TSUYAMA, S. MITAO and K. MINAKAWA, in "Microstructure/property relationships in titanium aluminides and alloys" (The Minerals, Metals, & Materials, 1991) p. 213.
23. K. S. CHAN and Y. W. KIM, *Met. Trans. A.* **23A** (1991) 1663.
24. Y. W. KIM, in " Microstructure/property relationships in titanium aluminides and alloys" (The Minerals, Metals, & Materials, 1991) p. 91.
25. S. SURESH, *Met. Trans. A* **16A** (1985) 249.
26. Y. MUTOH, M. TAKAHASHI, T. OIKAWA and H. OKAMOTO, in "Fatigue of advanced materials" (MCEP Ltd, 1991) p. 211.
27. G. R. YODER, L. A. COOLEY and T. W. CROOKER, in "Fracture mechanics; Fourteenth Symposium - Vol. 1, Theory and analysis, ASTM STP 791" (American Society of Testing Materials, 1983) p. 1.

Received 17 December 1992
and accepted 21 March 1994